Theory of triplet exciton polarons and photoinduced absorption in conjugated polymers

Yukihiro Shimoi* and Shuji Abe

Electrotechnical Laboratory, Umezono, Tsukuba 305, Japan

(Received 9 August 1993; revised manuscript received 14 December 1993)

Triplet exciton polarons in nondegenerate conjugated polymers are studied theoretically. Both electron-electron and electron-lattice interactions are taken into account in the Pariser-Parr-Pople model. The electronic and lattice structures of exciton polarons and their adiabatic energy surfaces are calculated by means of the unrestricted Hartree-Fock and the single-configuration-interaction methods. The calculated absorption spectrum of a triplet exciton polaron explains well the photoinduced absorption (PA) spectrum observed in polydiacetylene. An excitonic effect turns out to be crucial in explaining the narrow-peak profile of the observed PA spectrum. The present theory may well apply to the similar PA observed in poly(p-phenylene vinylene).

I. INTRODUCTION

Conjugated polymers have been widely investigated both theoretically and experimentally during the last decade.[1] In recent years, they have also attracted much attention as nonlinear optical materials. Due to the low-dimensional nature of their electronic and lattice structures, the ground state undergoes Peierls distortion and various nonlinear localized defects such as solitons, polarons, exciton polarons, and bipolarons are generated upon photoexcitation and doping. Many unusual properties of conjugate polymers have been considered to be associated with these excitations.

The photoinduced absorption (PA) spectrum provides fundamental information on excited states. It has been shown to be especially useful in order to understand the electronic structure of conjugated polymers.[2] A relatively narrow peak has been observed at about 1.4 eV in the PA spectrum of polydiacetylene (PDA),[3-5] which has been investigated most extensively among families of conjugated polymers with nondegenerate ground states. It has been established that the peak is associated with an optical transition from a triplet state.[6-9] A similar PA peak of triplet origin has been reported in poly(p-phenylene vinylene) (PPV) and its derivatives.[10-13]

On the other hand, there have been very few theoretical works on the triplet state and the PA spectrum of nondegenerate conjugated polymers.[9,14-16] Su[15] proposed that triplet neutral bipolarons (exciton polarons) are responsible for the PA peak in PDA. He calculated the absorption spectrum of the triplet state using the Su-Schrieffer-Heeger (SSH) model[17] with appropriate modifications for PDA.[18,19] The model includes an electron-lattice coupling but neglects electron-electron interactions. It turned out that the calculated absorption spectrum was in disagreement with the experiments: the calculated peak position 0.5 eV was much lower in energy than the observed one. Su speculated that the disagreement originated from the neglect of Coulomb interactions. By introducing the Hubbard on-site U in a perturbational method, he estimated that a U of about 12 eV is necessary to explain the 1-eV peak shift. Since this value of U is quite large, such a perturbational calculation may not be very reliable.

On the other hand, Abe, Yu, and Su[20] recently showed that the binding energy of a triplet exciton can be as large as 1 eV even for a relatively moderate interaction strength, if one takes into account the long-range nature of the electron-electron interaction by means of the Pariser-Parr-Pople (PPP) model.[21-23] The excitonic effect was taken into account within the single configuration-interaction (CI) method. Abe et al.[24-26] subsequently studied nonlinear optical spectra of the same model, finding good agreement between calculated and experimental spectra. The problem of excitons in conjugated polymers was surveyed in Refs. 27 and 28.

However, the excitons treated in these studies are *free* excitons on a perfect dimerized chain. To address the question of PA, the effect of lattice relaxation is considered to be significant. Therefore, both the electron-lattice interaction and the exciton effect must be taken into account. We have performed such a study for nondegenerate conjugate polymers. We used the PPP model with electron-lattice coupling of the SSH type, and treated the model by means of two different approximations: one is the unrestricted Hartree-Fock (UHF) method, and

the other is the single CI method as used in Refs. 20 and 24–26. We will demonstrate that one can obtain a qualitative picture of lattice relaxation of photoexcited states and photoinduced absorption in nondegenerate conjugated polymers. Furthermore, an interesting feature of the exciton polaron is obtained in the present study. In the CI method, the relevant excited state of a triplet exciton polaron turns out still to be an exciton trapped to the polaron deformation. In the SSH model and also in the UHF method, in contrast, the optical excitation of a triplet neutral bipolaron (exciton polaron) inevitably results in the "ionization" of the polaron: an electron or a hole is removed from the polaron level and becomes free, leaving a charged polaron behind. This has an important implication for the line shape of the PA spectrum. In the CI method, the single predominant exciton-exciton transition provides a narrow peak in the PA spectrum, accounting qualitatively for the observed spectra. On the other hand, in the case of the UHF calculation and the SSH model, the PA spectrum (in the limit of an infinitely long chain) intrinsically possesses a broad, asymmetric line shape because of the band character of the final states, although the disagreement of the peak position in the SSH model is improved by the UHF model.

In this paper, we consider a linear chain, and treat nondegeneracy by means of the so-called Brazovskii-Kirova (BK) model,[29] neglecting the triple bonds in PDA and the phenyl rings in PPV. The fact that similar triplet PA spectra have been observed commonly in the polymers with much different backbone structures suggests that the phenomenon is less sensitive to the individual structure. This partly justifies our use of the BK-type model, although limitation of the BK model has been pointed out.[30] We intend to give a unified picture for the PA phenomenon in nondegenerate polymers.

The rest of this paper is arranged as follows. In Sec. II, we briefly describe our model and calculation method. In Sec. III, we present the main results of our calculations. Roughly speaking, the two methods give similar results, but there are some important differences, as mentioned above. Concluding remarks are given in Sec. IV.

II. MODEL AND CALCULATION METHOD

To investigate the electronic structure of nondegenerate conjugate polymers, we adopt the PPP model for π electrons on a linear chain. It consists of the hopping term between nearest-neighbor sites, the on- and off-site Coulomb interactions, and the elastic energy of the lattice. The PPP Hamiltonian is given as

$$H = -\sum_{n,\sigma} t_{n,n+1}(C_{n+1,\sigma}^{\dagger}C_{n,\sigma} + C_{n,\sigma}^{\dagger}C_{n+1,\sigma})$$
$$+ \sum_n U\rho_{n\uparrow}\rho_{n\downarrow} + \sum_{n \neq m}\sum_{\sigma,\sigma'}\frac{V_{nm}}{2}\rho_{n,\sigma}\rho_{m,\sigma'}$$
$$+ \sum_n \frac{K}{2}(u_{n+1}-u_n)^2 . \tag{1}$$

Here, $C_{n,\sigma}^{\dagger}(C_{n,\sigma})$ creates (annihilates) a π electron with spin σ at site n, and $\rho_{n,\sigma} = C_{n,\sigma}^{\dagger}C_{n,\sigma}$. u_n is the lattice displacement at site n. The transfer integral $t_{n,n+1}$ includes

electron lattice coupling α of the SSH type and the symmetry-breaking term δt of the BK type as follows:

$$t_{n,n+1} = t - \alpha(u_{n+1}-u_n) + (-1)^n\delta t . \tag{2}$$

We assume the dependence of the Coulomb interaction V_{nm} on the distance as $V_{nm} = V/|n-m|$.

We are primarily interested in the lowest triplet state of the system. For this purpose we have treated the Hamiltonian in Eq. (1) with two different methods. One is the UHF approximation for the spin state $S_z = 1$, and the other is the single-CI approximation.

In the UHF method the Coulomb interaction is taken into account at a mean-field level. Since the UHF state is not in principle an eigenstate of the total spin operator S there is a possibility of contamination by higher spin components $(S > 1)$. Nevertheless, we use the term "triplet" for the UHF state with $S_z = 1$ in this paper. Excited states are calculated by use of the frozen orbital approximation.

In the CI method, we construct a basis by the states in which an electron is excited from an occupied orbital to an unoccupied one upon the singlet ground state calculated by the restricted Hartree-Fock (RHF) method. Triplet and excited singlet states are obtained by diagonalizing the Hamiltonian (1) within the basis. In this way, we can take into account excitonic effects beyond the mean-field approximation for excited states.

The lattice displacements u_n are treated within the adiabatic approximation. The equilibrium lattice deformation of the ground state is a perfect dimerization $u_n = (-1)^n u_0$ resulting from the Peierls instability and the term δt in Eq. (2). An excitation brings about polaronic lattice relaxation. In the UHF method, the lattice is optimized by using the Hellmann-Feynman force equilibrium condition

$$y_n = u_{n+1} - u_n = -\frac{2\alpha}{K}\left[p_n - \frac{1}{N}\sum_m p_m\right] . \tag{3}$$

Here, y_n denotes the change of bond length, $p_n = \sum_\sigma\langle C_{n+1,\sigma}^{\dagger}C_{n,\sigma}\rangle$ is the bond order, and N is the total number of sites. The last term in Eq. (3) ensures $\sum_n y_n = 0$. In the CI calculation, it requires much computer time to determine the fully optimized lattice deformation in contrast to the UHF calculation, so that we assume the following expression of the lattice deformation:

$$u_n = (-1)^n u_n' , \tag{4a}$$

$$u_n' = u_0[1 - Q \, \text{sech}\{(n - n_C - \tfrac{1}{2})/\xi\}] . \tag{4b}$$

Here Q and ξ denote the amplitude and width of the deformation, respectively. The center of the exciton is located at the bond center between the n_Cth and (n_C+1)th sites.

The calculated electronic states are classified by their symmetries as follows. The lattice deformation given by Eq. (4) preserves the C_{2h} symmetry around the center of an exciton polaron. The many-body wave functions are classified as A_g or B_u states. Furthermore, the system possesses alternancy symmetry.[31] We add the superscript + or − according to Pariser's notation.[31]

In order to calculate the PA spectrum, we compute the matrix element P_m of the dipole moment between the lowest triplet state $|T_0\rangle$ and its mth optically allowed excited state $|T_m\rangle$: $P_m = -e\langle T_0|\sum_{n,\sigma}x_n\rho_{n,\sigma}|T_m\rangle$. Here x_n is the position of the nth site and e is the elementary electric charge. Since in our calculation $|T_0\rangle$ belongs to the $^3B_u^+$ symmetry, $|T_m\rangle$ must be a $^3A_g^-$ state. The absorption intensity at photon energy ω is proportional to $\sum_m\omega|P_m|^2\delta(E_m-\omega)$. Here E_m is the excitation energy of the state $|T_m\rangle$.

We have calculated the PA spectrum in addition to the various nonlinear optical spectra reported in Refs. 24–28 by use of the CI method, and found that the corresponding experiments in PDA can be well explained by using the following parameters: $t=1.65$ eV, $\delta t=0.05t$, $U=3.0t$, $V=1.3t$, $\alpha=4.2$ eV/Å, and $K=50$ eV/Å². These parameters give $u_0=0.024$ Å. The strength of the Coulomb interaction is intermediate, although the ratios V/t and U/V are somewhat larger than those used in Refs. 24–28. Note that δt in these references corresponds to $2\alpha u_0+\delta t$ in the present paper. In Sec. III we show results calculated with these parameters. Numerical calculations have been performed for the system of half-filling with $N=100$. We impose the periodic boundary condition.

III. RESULTS

A. UHF calculation

We begin with results obtained in the UHF approximation. In Fig. 1, we display the lattice and electronic structures of a triplet exciton polaron, with the lattice being fully optimized by using the Hellmann-Feynman force equilibrium condition of Eq. (3). The electronic state has B_u symmetry. In Figs. 1(a), 1(b), and 1(c), we depict the alternating bond variable $\tilde{y}_n$ $=(-1)^{n+1}y_n/2u_0$, the bond order p_n, and the spin density $s_n=(\langle\rho_{n,\uparrow}\rangle-\langle\rho_{n,\downarrow}\rangle)/2$, respectively. All of them indicate that the exciton polaron is localized with a width of about ten sites. The deviations of $\tilde{y}_n$ and p_n from the background regular bond-order wave (BOW) are so large as to reverse the phases of alternating patterns at the central region of the exciton. As shown in Fig. 1(c), negative spin densities appear at every two sites, giving a strongly
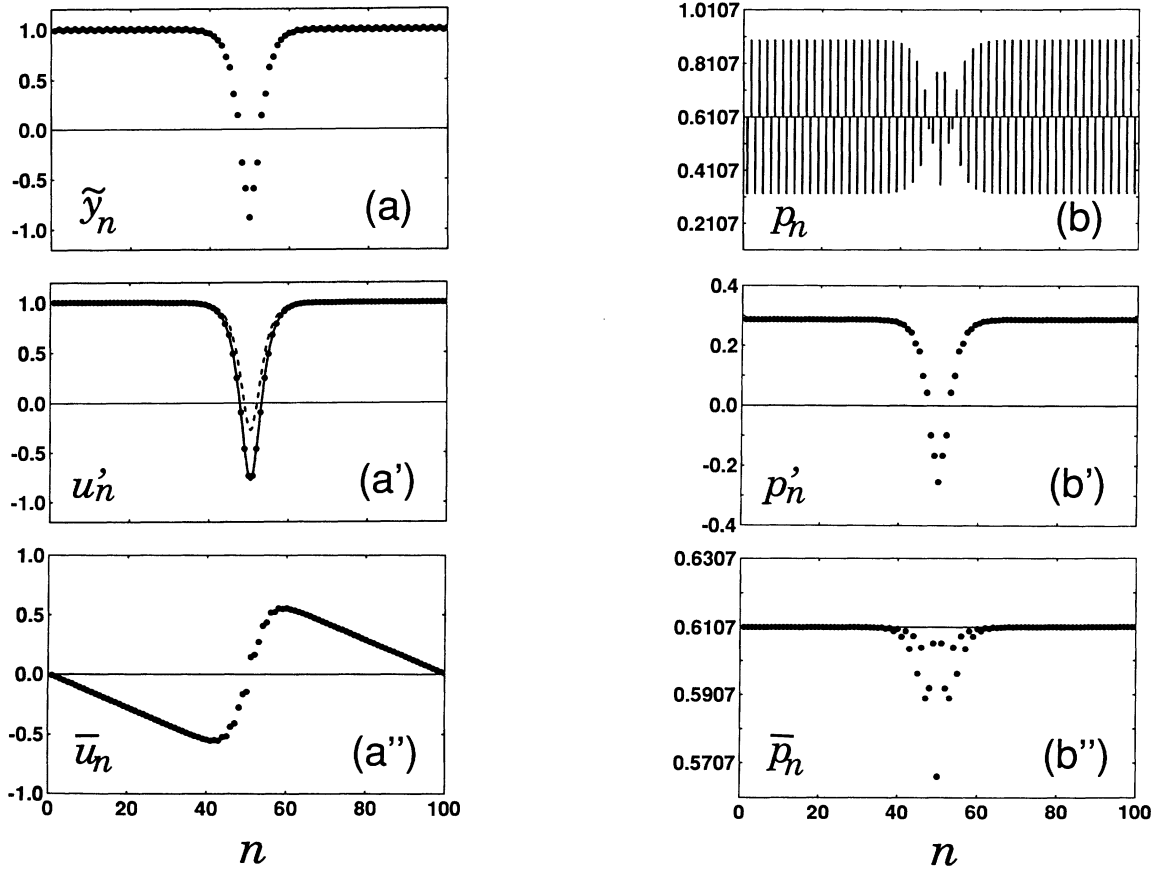

FIG. 1. Lattice and electronic structures of a triplet exciton polaron obtained by the UHF method. (a), (a'), and (a'') display the alternating bond variable $\tilde{y}_n$ and the alternating and nonalternating components u_n' and $\bar{u}_n$ of the lattice deformation, respectively. u_n' and $\bar{u}_n$ are normalized by u_0 (=0.02416 Å). A solid curve in (a') indicates Eq. (4.b) fitted to the UHF calculation ($Q=1.78$ and $\xi=2.32$). The dashed one shows Eq. (4.b) giving the energy minimum in the CI calculation ($Q=1.27$ and $\xi=2.25$). The bond order p_n (the spin density s_n) and its alternating and nonalternating components p_n' and $\bar{p}_n$ (s_n' and $\bar{s}_n$) are shown in (b), (b'), [(c), (c'), and (c'')], respectively. The lattice deformation is fully optimized by the Hellmann-Feynman force equilibrium condition [Eq. (3)].
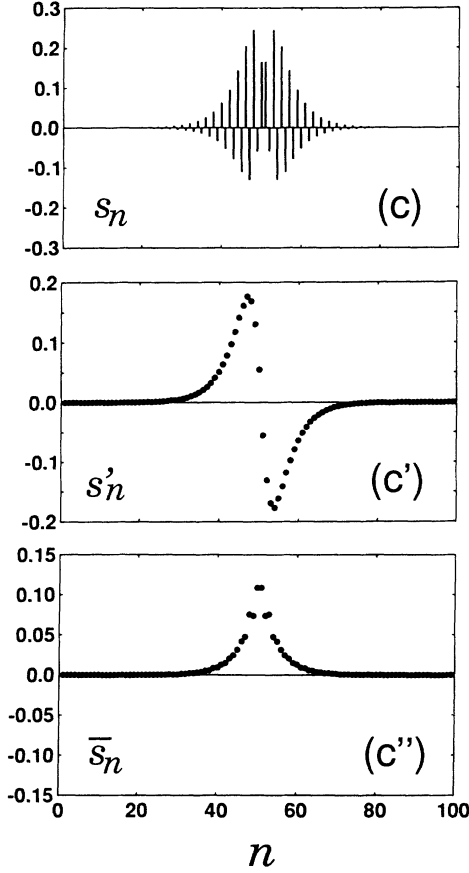
FIG. 1. (Continued).

$$p_n = \bar{p}_n + (-1)^n p_n' \ ,$$

$$s_n = \bar{s}_n + (-1)^n s_n' \ ,$$

$$\bar{p}_n = (p_{n-1} + 2p_n + p_{n+1})/4 \ ,$$

$$\bar{s}_n = (s_{n-1} + 2s_n + s_{n+1})/4 \ .$$

(6)

These are depicted in Figs. 1(b'), 1(c'), 1(b''), and 1(c''). p_n' is smooth and similar to u_n'. $\bar{p}_n$ decreases slightly at the central region, corresponding to a local expansion of the lattice as indicated by $\bar{u}_n$. Both s_n' and $\bar{s}_n$ have smooth profiles. The amplitude of s_n' is larger than that of $\bar{s}_n$. These characteristics are similar to those of the polaron case in Ref. 32.

The exciton polaron shown in Fig. 1 is centered at a short bond of the background BOW. We can obtain another type of exciton polaron which is centered at a long bond. It has a slightly higher energy (by $0.00043t$). The two types of exciton differ in the signs of alternating components, as pointed out for solitons and polarons in Ref. 32. (Lifting of the degeneracy between states with opposite signs of alternating components is discussed in Ref. 34).

Figure 2 shows the energy-level structure of the exciton-polaron state given in Fig. 1. It is characterized by an in-gap orbital for each spin localized spatially around the central region of the exciton. The orbital corresponds to the highest occupied molecular orbital (HOMO) for the up-spin and the lowest unoccupied MO (LUMO) for the down-spin. We obtain localized orbitals even in the case of a perfect dimerized lattice. In the SSH model, an exciton-polaron state has two in-gap states. In our calculation, the existence of the second in-gap state is not clear, since the second HOMO and LUMO lie near the edge of the band in energy, and their wave functions are fairly extended in space.

In Fig. 3, the energy of the triplet exciton polaron is plotted by a thick solid curve, assuming the deformation

alternating pattern. s_n has a dip at the central region and maxima at the third site from the center of the exciton. Such a profile of spin density has also been found in a charged polaron state in the PPP-UHF model for polyacetylene.[32] The exciton polaron does not have the charge density and spin bond order.

As shown in Fig. 1(a), $\tilde{y}_n$ has small ripples outside the central region. They come from the slowly varying, nonalternating component of u_n. The existence of such a component has been pointed out for solitons and polarons in the SSH model.[33] We decompose u_n into alternating and nonalternating components u_n' and $\bar{u}_n$ as

$$u_n = \bar{u}_n + (-1)^n u_n' \ ,$$

$$\bar{u}_n = (u_{n-1} + 2u_n + u_{n+1})/4 \ .$$

(5)

They are plotted in Figs. 1(a') and 1(a''). u_n' is smooth and well fitted by the expression given in Eq. (4b) with $Q = 1.78$ and $\xi = 2.32$. The fitted curve is depicted by the solid line in Fig. 1(a'). $\bar{u}_n$ has a magnitude similar to that of u_n'. Its behavior in Fig. 1(a'') corresponds to a local expansion of the lattice around the exciton polaron. This is opposite to the charged-polaron case, where the lattice contracts locally (Ref. 33). We also decompose p_n and s_n into alternating components p_n' and s_n' and nonalternating ones $\bar{p}_n$ and $\bar{s}_n$ as
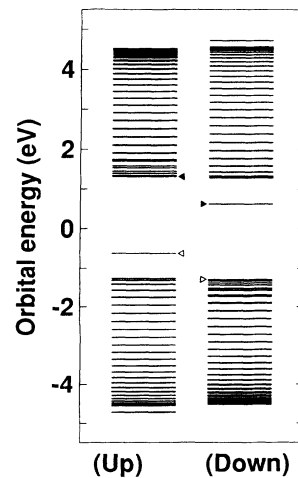

FIG. 2. The energy-level structure of up- and down-spin electrons for the triplet exciton polaron state calculated by the UHF method and given in Fig. 1. Open (solid) triangles indicate the HOMO (LUMO) orbitals for each spin.
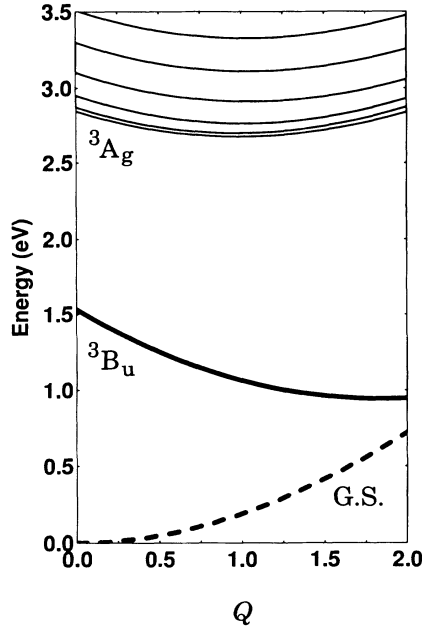
FIG. 3. Adiabatic energy potentials against Q for the triplet states obtained by the UHF method. The thick solid curve shows the lowest triplet branch, which has the excitonic character with ^3B_u symmetry. The other solid curves indicate ^3A_g excited states. The singlet ground state is also indicated by the thick dashed line. The value of ξ is fixed to 2.25.

given by Eq. (4) with $\xi = 2.25$. The nonalternating component $\bar{u}_n$ is neglected, since it gives only ripples in $\bar{y}_n$ and is not considered to play an important role in the electronic structure. In addition, we plot in Fig. 3 the energies of excited states with ^3A_g symmetry which are accessible from the lowest triplet state via dipole transitions. The thick dashed curve represents the singlet A_g ground state.

The branch of the lowest triplet state is separated in energy from the excited ones, even in the case of $Q = 0$. It is similar to that obtained by the CI method, as shown below (Fig. 7). This implies that the excitonic effect between an electron and a hole is partly taken into account in the UHF calculation through the formation of the localized in-gap orbitals. However, this effect is not taken into account for the excited A_g states in the UHF method. The energy minimum of the lowest triplet state in Fig. 3 is located at about $Q = 1.8$, which is very close to the value $Q = 1.78$ obtained by fitting Eq. (4.b) with the fully optimized lattice deformation u_n'. The difference between the energy at $Q = 1.8$ and that of the fully optimized lattice is only $0.001t$. Therefore, the assumed expression, Eq. (4), of the lattice deformation seems adequate.

The excited states shown in Fig. 3 are obtained by exciting an electron from the localized gap level to the bandlike states extending over the entire chain. They are discrete in energy due to the finite size in our calculation. There is no excitonic state other than the lowest triplet state, in contrast to the result of the CI method, as will be described below. Excitations from the valence to the conduction bands are omitted in Fig. 3. They need larger
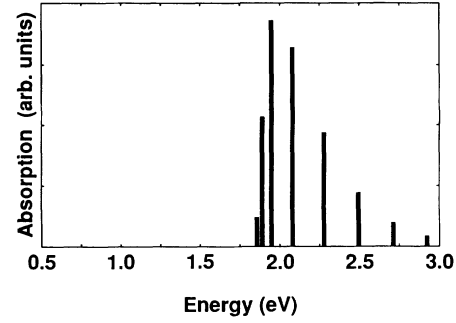

FIG. 4. The triplet-triplet absorption spectrum calculated by the UHF method. The initial state is the lowest triplet state with the fully relaxed lattice configuration. Transitions only from or to the localized gap states are only taken into account.

energies and have energy curves parallel to that of the lowest triplet state. The lowest one among them has an energy of about 3.25 eV at $Q = 2.0$.

Figure 4 shows the absorption spectrum of the triplet exciton-polaron state with the fully relaxed lattice given in Fig. 1. We only take account of the excitations from or to the localized in-gap state, since those from the valence to the conduction bands give an absorption spectrum similar to the regular BOW and do not contribute to the PA. The absorption is strongest at about 2.0 eV,
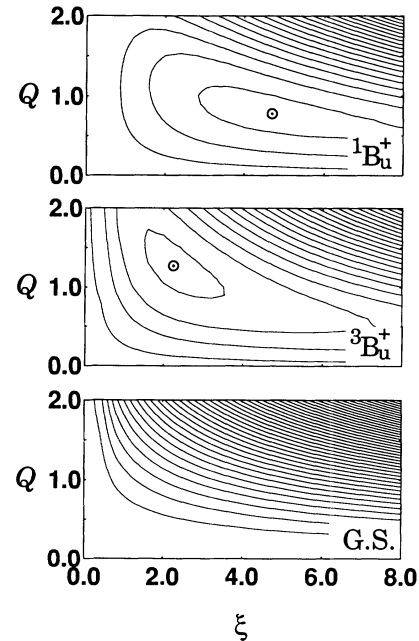

FIG. 5. Contour diagrams of adiabatic potential surfaces of (from bottom to top) the singlet ground state (GS), the lowest triplet B_u exciton state ($^3B_u^+$), and the lowest singlet one ($^1B_u^+$), in the parameter space defined by Q and ξ in Eq. (4). The singlet ground state is obtained by the RHF method and the excitonic states are obtained by the single-CI calculation. The circled dots indicate energy minima. The center of the polaron deformation is located at a short bond of the background BOW. The deformation centered at a long bond gives energy minima at approximately the same positions as that centered at a short bond with almost degenerate energies.

YUKIHIRO SHIMOI AND SHUJI ABE

and decreases gradually with increasing energy, resulting in an overall asymmetric profile. The discreteness of bars in Fig. 4 is due to our finite-size calculation. In the infinite system, the spectrum should become a broad band with a peak and a continuous tail, similar to that obtained by the SSH model.[15] The maximum absorption in Fig. 4 lies at an energy higher than the observed peak position 1.4 eV.[3−5,10−13] By using somewhat smaller U and V, the peak position can be shifted to about 1.4 eV, while the overall profile remains essentially the same.

B. CI calculation

Next, we present the results obtained by the single-CI calculation. We assume the lattice deformation given in Eq. (4). Figure 5, from bottom to top, shows contour diagrams of the energies of the singlet ground state, and the lowest triplet and singlet excitonic states in the parameter space defined by Q and ξ in Eq. (4). The three states belong to the $^1A_g^-$, $^3B_u^+$ and $^1B_u^+$ symmetries, respectively. The energy of the singlet ground state obtained by the RHF method increases with increasing Q and ξ. Exciton states are stabilized by relaxing the lattice locally, forming exciton polarons. The triplet exciton has a rather shallow energy minimum at $Q=1.27$ and $\xi=2.25$, which is depicted by a circle with dot in Fig. 5. The energy at

this point is slightly higher (by $0.04t$) than that obtained by means of the UHF method with full optimization. We plot u_n' for these parameters by a dashed line in Fig. 1(a') to compare the lattice structures obtained by the CI and UHF methods. The value of Q in the CI method is smaller than that in the UHF case, implying that the local deformation is smaller. The singlet exciton has an energy minimum at a larger ξ, and a smaller Q than those for the triplet one as shown in Fig. 5.

Figure 6 shows the real-space electronic structure of the triplet exciton-polaron state with the stable structure ($Q=1.27$ and $\xi=2.25$). The bond order p_n (spin density s_n), and its alternating and nonalternating components p_n' and $\bar{p}_n$ (s_n' and $\bar{s}_n$) are depicted in Figs. 6(a)–6(a'') [6(b)–6(b'')]. The deviation of p_n from the background regular BOW is smaller than that in the UHF calculation (Fig. 1), and p_n' is negative only at the center with a very small absolute value. $\bar{p}_n$ decreases slightly in the central region, as seen in the UHF case [Figs. 6(a'') and 1(b'')].

The single-CI method always makes the spin density positive [Fig. 6(b)] with total sum $\sum_n s_n = 1$. This tends to suppress the magnitude of the spin density compared to that calculated by the UHF method. The amplitudes of s_n' in Fig. 6(b') are about one fifth of those in the UHF in Fig. 1(c'), although their overall line shapes are similar.
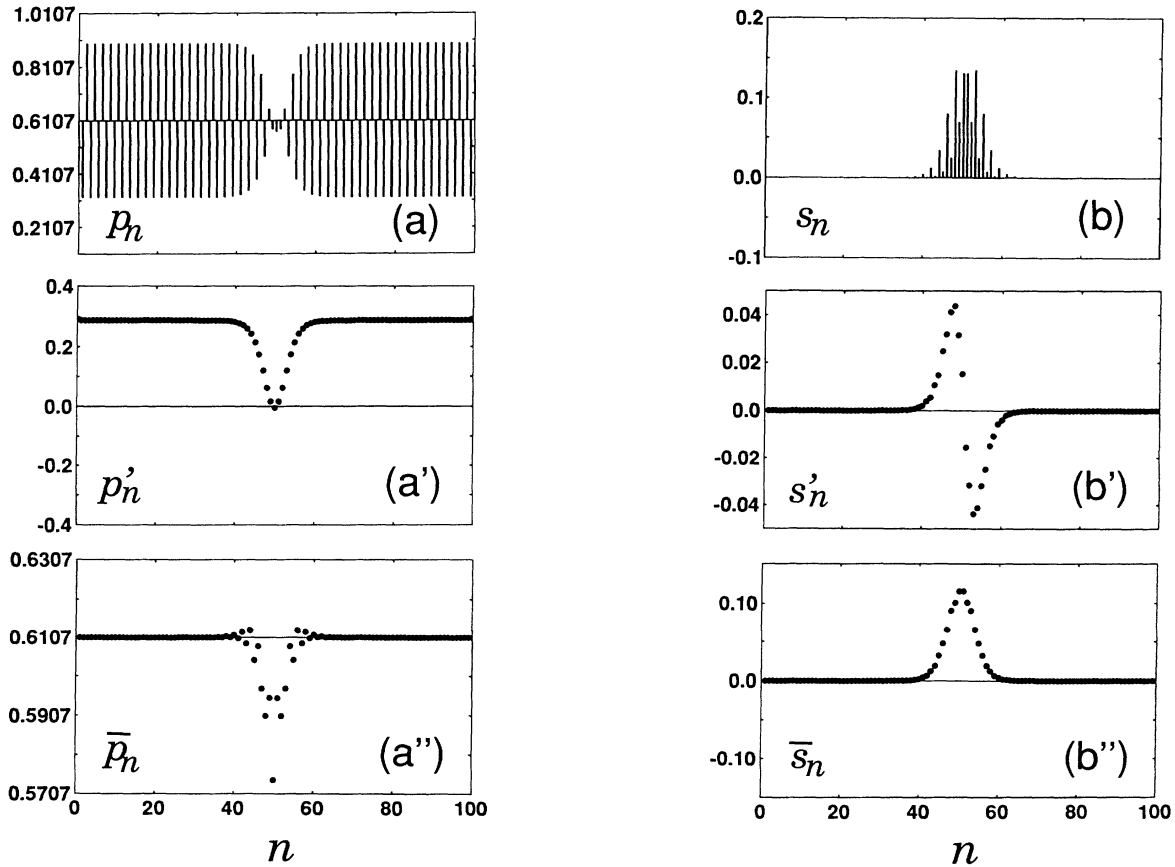

FIG. 6. The electronic structure of a triplet exciton polaron obtained by the CI calculation. The bond order p_n (the spin density s_n) and its alternating and nonalternating components p_n' and $\bar{p}_n$ (s_n' and $\bar{s}_n$) are shown in (a), (a'), and (a'') [(b), (b'), and (b'')], respectively. The lattice deformation is optimized within Eq. (4) with $Q=1.27$ and $\xi=2.25$.
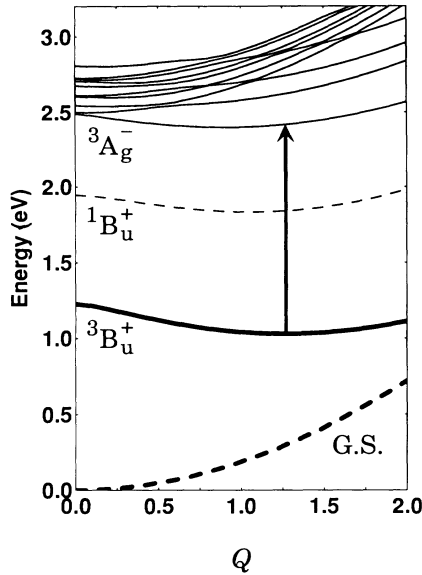
FIG. 7. Adiabatic energy potentials against Q obtained by the CI calculation. The thick solid line (the thin dashed line) represents the lowest triplet (singlet) excitonic state with B_u^+ symmetry. The thick dashed line indicates the $^1A_g^-$ ground state obtained by the RHF method. The thin solid lines are the lowest ten A_g^- states, which are degenerate for spin singlet and triplet. The value of ξ is fixed to 2.25.

In Fig. 7, we present the energy surfaces for several states relevant to the PA and linear absorption. It is plotted against Q with the value of ξ fixed at 2.25. The branches of the lowest triplet and singlet excitonic states with B_u^+ symmetry are shown by thick solid and thin dashed lines, respectively. The thin solid lines indicate $^3A_g^-$ excited states. The $^1A_g^-$ ground state (thick dashed line) obtained by the RHF method is the same as that in Fig. 3.

The nature of the excited $^3A_g^-$ states in Fig. 7 is as follows. The lowest $^3A_g^-$ state has an excitonic character. This state was not obtained in the UHF method. At $Q=0$, free-electron-hole states begin at about 2.5 eV. They have energy curves parallel to that of the singlet ground state. A few branches come off the free-electron-hole continuum with increasing Q. In these states, either an electron or a hole is delocalized, but the other carrier is captured at the local deformation, forming a polaron.

At $Q=0$ the lowest triplet and singlet excitons have large binding energies (about 1.3 and 0.6 eV, respectively, on the basis of the bottom of the free-electron-hole continuum at about 2.5 eV). These energies are purely of electronic origin. With increasing Q, the exciton states are stabilized by the polaron effect, whereas free-electron-hole states do not have such an effect and require only the elastic deformation energy. Therefore, the binding energies increase with increasing Q, as shown in Fig. 7.

The absorption spectrum of the triplet B_u^+ exciton polaron obtained in the single CI is shown by solid bars in the lower panel of Fig. 8. The broken bar is the linear absorption spectrum of the singlet ground state with the perfect dimerized lattice ($Q=0$). The latter has a peak at
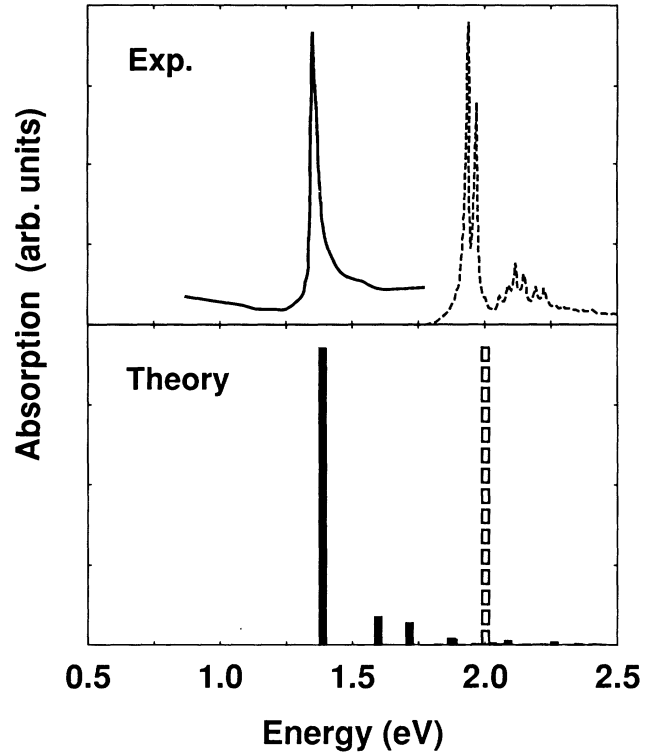

FIG. 8. Absorption spectra obtained by the CI calculation (lower panel) in comparison with observed ones (upper panel). In the lower panel, solid bars represent the spectrum of the triplet B_u^+ exciton polaron state with the optimized lattice structure ($Q=1.27$ and $\xi=2.25$). In contrast to the results of the UHF calculation (Fig. 4), the spectrum is dominated by a single transition indicated by an arrow in Fig. 7. The broken bar indicates the linear absorption spectrum of the singlet A_g^- ground state with perfect dimerized lattice ($Q=0$). In the upper panel, the solid and broken lines indicate the PA (Ref. 4) and the linear absorption (Ref. 35) spectra of PDA (more precisely, poly[2,4-hexadiyne-1,6-diol-bis(p-toluene sulfonate)], or PTS) observed at low temperatures, respectively. In both the upper and lower panels, the relative intensities of the PA and the linear absorption are arbitrary.

~2 eV for the parameters used, matching the main absorption feature of a PDA single crystal[35] shown by the broken line in the upper panel of Fig. 8. (The splitting of the main peak is due to inequivalent chains in the crystal. The weak features above 2 eV are phonon sidebands, which are not taken into account in the present calculations.)

The calculated triplet absorption spectrum is dominated by a single transition, in contrast to the results of the UHF calculation (Fig. 4), where the spectrum (in the limit of an infinitely long chain) intrinsically possesses a broad, asymmetric line shape because of the band character of the final states. The dominant transition is indicated by an arrow in Fig. 7, its final state being the lowest $^3A_g^-$ excited state that has an excitonic character. It occupies a large oscillator strength because of a large overlap of wave functions between the initial and final states. The weak absorption peaks at higher energies come from transitions to higher $^3A_g^-$ states in which either an elec-

tron or a hole is delocalized. These transitions are similar to those obtained by the UHF method. The difference in the peak profile between the CI and UHF methods arises from the existence of the excitonic A_g^- state in the CI method.

The solid line in the upper panel of Fig. 8 represents the PA spectrum observed in a PDA crystal at a low temperature by Hattori, Hayes, and Bloor.[4] The calculated spectrum in the lower panel reproduces the observed PA spectrum quite well in both the peak position and the spectral profile. The sharpness of the observed PA peak cannot be explained by the UHF result in Fig. 4 as well as by the result of the noninteracting model.[15] We have compared our results with experimental data for single crystals at low temperature, because our calculations are for zero temperature and do not take account of disorder effects. The PA spectrum is much broader at higher temperatures or in the presence of large disorder.[3,4,8,13]

In PPV, the observed PA peak is located at a position similar to that of PDA, while the linear absorption peak is located somewhat higher in energy than that of PDA.[10,13] These observations can essentially be explained by the energy diagram shown in Fig. 7, with slightly shifting the curves of all the excited states upwards relative to the ground state. Such a modification is possible by using a somewhat larger δt than in the case of PDA. However, the situation is less clear about the nature of the PA in PPV, because the observed peak is broader than in PDA. Although there is a tendency to narrow with improving sample quality,[13] it is not clear at present whether the width is intrinsic or still affected by disorder.

IV. CONCLUDING REMARKS

In this paper, we have studied the model in which both electron-lattice and long-range electron-electron interactions are taken into account. This model is a natural extension of the previous model used in Refs. 20 and 24–28. We have shown that the picture of a triplet exci-

ton polaron within the single-CI treatment of the PPP model provides a good description of the PA spectra for PDA and presumably also for PPV. First, the Coulomb interaction improves the discrepancy between the observed PA peak position and the result of the SSH model. This is also possible at the UHF level, which effectively includes exciton effects in the triplet ground state by forming localized orbitals. Second, as for the profile of the PA spectrum, the excitonic character of excited states is crucial in our calculation to give a single strong peak.

The UHF and single-CI methods give similar results for the energy surfaces of ^3B_u exciton polarons, as shown in Figs. 3 and 7. However, the detailed electronic and lattice structures of the exciton polaron are different in the two methods: e.g., the existence of the negative spin density. We hope that the detailed structures will be clarified by experiments such as the electron-nuclear double-resonance (ENDOR) technique.[36]

In PPV, some experiments have indicated the existence of PA peaks associated with bipolarons.[10,12] However, these have not been observed in an improved sample of PPV nor in one of its derivatives.[13,11] From a theoretical point of view, the intrinsic photogeneration of a bipolaron seems difficult because of Coulomb repulsion between charged objects with the same sign.

It has been observed that a photoexcited singlet exciton relaxes to a self-trapped state (a singlet exciton polaron) with a time constant of about 150 fs, and that its lifetime is about 2.0 ps.[37,38] Relaxation processes from photoexcited singlet excitons or electron-hole pairs to singlet or triplet exciton polarons are an interesting problem to study based on the present work.

ACKNOWLEDGMENTS

*Electronic address: e9313@etlrips.etl.go.jp

[1]For a recent review, see, for instance, Conjugated Conducting Polymers, edited by H. G. Kiess, Springer Series in Solid State Sciences Vol. 102 (Springer-Verlag, Berlin, 1992).

[2]R. H. Friend, D. D. C. Bradley, and P. D. Townsend, J. Phys. D 20, 1367 (1987).

[3]J. Orenstein, S. Etemad, and G. L. Baker, J. Phys. C 17, L297 (1984).

[4]T. Hattori, W. Hayes, and D. Bloor, J. Phys. C 17, L881 (1984).

[5]B. I. Greene, J. Orenstein, R. R. Millard, and L. R. Williams, Chem. Phys. Lett. 139, 381 (1987).

[6]L. Robins, J. Orenstein, and R. Superfine, Phys. Rev. Lett. 56, 1850 (1986).

[7]M. Winter, A. Grupp, M. Mehring, and H. Sixl, Chem. Phys. Lett. 133, 482 (1987).

[8]H. Sixl, R. Jost, and R. Warta, J. Chem. Phys. 87, 4429 (1987).

[9]C. Kollmar, W. Rühle, J. Frick, H. Sixl, and J. U. v. Schütz, J. Chem. Phys. 89, 55 (1988).

[10]N. F. Colaneri, D. D. C. Bradley, R. H. Friend, P. L. Burn, A. B. Holmes, and C. W. Spangler, Phys. Rev. B 42, 11 670 (1990).

[11]L. Smilowitz and A. J. Heeger, Synth. Met. 48, 193 (1992).

[12]H. S. Woo, S. C. Graham, D. A. Halliday, D. D. C. Bradley, R. H. Friend, P. L. Burn, and A. B. Holmes, Phys. Rev. B 46, 7379 (1992).

[13]K. Pichler, D. A. Halliday, D. D. C. Bradley, P. L. Burn, R. H. Friend, and A. B. Holmes, J. Phys. Condens. Matter 5, 7155 (1993).

[14]D. R. Yarkony, Chem. Phys. 33, 171 (1978).

[15]W. P. Su, Phys. Rev. B 36, 6040 (1987).

[16]H. Tanaka, M. Inoue, and E. Hanamura, Solid State Commun. 63, 103 (1987).

[17]W. P. Su, J. R. Schrieffer, and A. J. Heeger, Phys. Rev. Lett. 42, 1698 (1979).

[18]C. Cojan, C. P. Agrawal, and C. Flytzanis, Phys. Rev. B 15, 909 (1977).

[19]N. A. Cade and B. Movaghar, J. Phys. C 16, 539 (1983).

[20]S. Abe, J. Yu, and W. P. Su, Phys. Rev. B 45, 8264 (1992).

[21]R. Pariser and R. G. Parr, J. Chem. Phys. 21, 466 (1953).

[22]R. Pariser and R. G. Parr, J. Chem. Phys. 21, 767 (1953).

[23]J. A. Pople, Trans. Faraday Soc. 49, 1375 (1953).

[24]S. Abe, M. Schreiber, W. P. Su, and J. Yu, Phys. Rev. B 45, 9432 (1992).

[25]S. Abe, M. Schreiber, W. P. Su, and J. Yu, J. Lumin. 53, 519

(1992).

[26] S. Abe, M. Schreiber, W. P. Su, and J. Yu, Mol. Cryst. Liq. Cryst. **217**, 1 (1992).

[27] S. Abe, Prog. Theor. Phys. Suppl. **113**, 83 (1993).

[28] S. Abe, in *Relaxation in Polymers,* edited by T. Kobayashi (World Scientific, Singapore, 1993), p. 215.

[29] S. A. Brazovskii and N. N. Kirova, Pis'ma Zh. Eksp. Teor. Fiz. **33**, 6 (1981) [JETP Lett. **33**, 4 (1981)].

[30] H. Y. Choi and M. J. Rice, Phys. Rev. B **44**, 10 521 (1991).

[31] R. Pariser, J. Chem. Phys. **24**, 250 (1956).

[32] A. Takahashi and H. Fukutome, Solid State Commun. **62**, 279

(1987).

[33] A. Terai and Y. Ono, J. Phys. Soc. Jpn. **55**, 213 (1986).

[34] Y. Shimoi and H. Fukutome, Solid State Commun. **82**, 407 (1992).

[35] G. Weiser, Phys. Rev. B **45**, 14 076 (1992).

[36] S. Kuroda and H. Shirakawa, Phys. Rev. B **35**, 9380 (1987).

[37] M. Yoshizawa, M. Taiji, and T. Kobayashi, IEEE J. Quantum Electron. **25**, 2532 (1989).

[38] M. Yoshizawa, A. Yasuda, and T. Kobayashi, Appl. Phys. B **53**, 296 (1991).